

Effects of Valproic Acid, a Histone Deacetylase Inhibitor, on improvement of Locomotor Function in Rat Spinal Cord Injury Based on Epigenetic Science

Alireza Abdanipour^{*1,3}, Hermann J. Schluesener² and Taki Tiraihi³

¹Stem Cells Research Laboratory, Dept. of Medical Sciences, Ardabil Branch, Islamic Azad University, Ardabil, Iran;

²Division of Immunopathology of the Nervous System, Tuebingen University, Germany;

³Dept. of Anatomical Sciences, School of Medical Sciences, Tarbiat Modares University, and Shefa Neurosciences Research Center, Khatam Al-Anbia Hospital, Tehran, Iran.

Received 11 December 2011; revised 10 January 2012; accepted 11 January 2012

ABSTRACT

Background: The primary phase of traumatic spinal cord injury (SCI) starts by a complex local inflammatory reaction such as secretion of pro-inflammatory cytokines from microglia and injured cells that substantially contribute to exacerbating pathogenic events in secondary phase. Valproic acid (VPA) is a histone deacetylase inhibitor. Acetylation of histones is critical to cellular inflammatory and repair processes. **Methods:** In this study, rats were randomly assigned to five experimental groups (laminectomy, untreated, and three VPA-treated groups). For SCI, severe contusion was used. In treated groups, VPA was administered intraperitoneally at doses of 100, 200 and 400 mg/kg daily three hours after injury for 7 days. To compare locomotor improvement among experimental groups, behavioral assessments were performed by the Basso, Beattie and Bresnahan (BBB) rating scale. The expression of neurotrophins was evaluated by RT-PCR and real-time PCR. **Results:** VPA administration increased regional brain-derived neurotrophic factor and glial cell-derived neurotrophic factor mRNA levels. Local inflammation and the expression of the lysosomal marker ED1 by activated macrophages/microglial cells were reduced by VPA and immunoreactivity of acetylated histone and microtubule-associated protein were increased. **Conclusion:** The results showed a reduction in the development of secondary damage in rat spinal cord trauma with an improvement in the open field test (BBB scale) with rapid recovery. *Iran. Biomed. J. 16 (2): 90-100, 2012*

Keywords: Inflammation, Epigenetics, Valproic acid (VPA)

INTRODUCTION

The important topic in spinal cord injury (SCI) is inflammation. Inflammation and overactivation of the inflammatory response in earlier stage have important roles in secondary phase. The primary phase of traumatic SCI starts by a complex local inflammatory reaction such as secretion of pro-inflammatory cytokines from microglia and injured cells that substantially contribute to exacerbating pathogenic events in secondary phase. In primary phase, because of secretion of pro-inflammatory cytokines (IL-1 β , IL-6 and tumor necrosis factor- α) a cascade of immune reaction occurs that persists for several weeks and leads to secondary pathogenic events [1]. Valproic acid (VPA, 2-propylpentanoic acid) is a short-chain branched fatty acid, which is easily delivered into the organism and cells. VPA is a histone deacetylase (HDAC1) inhibitor modulating the

acetylation of histones and chromatin structure [2, 3]. Modification of chromatin structure regulates gene expression that contributes to the inflammatory process such as ED1. ED1 is a cellular marker specific for activated rat microglia, monocytes, and macrophages. It can be immunostained to show the presence of an immunological response in rats [4]. In addition to HDAC1 inhibition, VPA has some effects on voltage-gated sodium channels and might inhibit GABA transaminase. VPA also contributes to regeneration of damaged neurons via increasing mRNA and protein levels of neurotrophins, such as brain-derived neurotrophic factor (BDNF) and glial cell-derived neurotrophic factor (GDNF) in astrocytes. VPA is used clinically as a drug for treatment of epilepsy or bipolar disorder [5-7]. In animal models, VPA increased neurite outgrowth [8], axonal remodeling [9] and neurogenesis in the hippocampus [10]. Considering the promising background of clinical application of the

drug and its potential for the treatment of neurodegenerative conditions, we decided to study the effect of VPA in rat SCI.

MATERIALS AND METHODS

Animals and study design. Female Sprague-Dawley rats (250-350 g, Pasteur Institute of Iran, Tehran) were housed under standard conditions of humidity and temperature with 12 h light:12 h dark cycles and unlimited access to food and water. All procedures were approved by the Animal Care and Use Committee of Tarbiat Modares University (Tehran, Iran). The rats were randomly assigned to five experimental groups (n = 6 for each group) as follows: 1) laminectomy group; 2) untreated SCI group; 3) 100 mg/kg vPA-treated SCI group; 4) 200 mg/kg VPA-treated SCI group and 5) 400 mg/kg VPA-treated SCI group. For histopathological analysis, the rats were sacrificed 28 days post injury.

Rat spinal cord injury contusion model. Sever contusion SCI model was performed by a standard procedure [11]. Briefly, rats were anaesthetized by an intraperitoneal injection of 80 mg/kg ketamine and 5 mg/kg xylazine. After shaving, laminectomy was performed at the T12-L1 level and the exposed spinal cord was lesioned by a 10-g metal rod with a 2 mm diameter dropped from a height of 25 mm [12]. Then, the wound was closed by suturing muscles and skin layer by layer. Following surgery, the recovery of the animals was assisted by subcutaneous injection of 10 ml lactated Ringer's solution. Postoperative care such as manual bladder expression and intramuscular injection of 50 mg/kg cefazolin antibiotic were carried out twice daily for one week (Jabir Ibn Hayan, Tehran, Iran) [13].

Drug administration. Treatment groups received intraperitoneally 100, 200 and 400 mg/kg VPA daily for 7 days; started three hours after injury. VPA was dissolved in sterile saline to a final concentration of 60 mg/ml (for the 200 and 400 mg/kg doses) and 15

mg/ml (for the ≤ 100 mg/kg dose) [14].

Behavioral assessment. To compare locomotor improvement among experimental groups, behavioral assessments were performed by the Basso, Beattie and Bresnahan (BBB) rating scale [15] from zero (paralysis) to 21 points (normal gait). Rats were individually videotaped for four minutes by four digital video cameras, located inside a plastic container with 110 cm diameter and 50 cm height at 3, 7, 14, 21 and 28 days post SCI. During the evaluation, animals were allowed to walk freely on an open field surface. Two examiners, blinded to the treatment of rats, rated the rats and the mean core value of both ratings was recorded. Significant differences of scores were established by repeated measures analysis of variance (ANOVA), followed by Tukey's test post hoc analysis.

Reverse transcriptase-polymerase chain reaction (RT-PCR). The expression of neurotrophins (BDNF, GDNF) in 400 mg/kg VPA and untreated-SCI groups were evaluated by RT-PCR. The primers used in the study have been presented in Table 1. Purelink™ RNA mini kit (Invitrogen™) was used for extracting total RNA [16]. To obtain purified RNA, the extracted RNA was treated by DNaseI (Invitrogen™) and purified RNA was analyzed by spectroscopy and agarose gel electrophoresis. Afterward, according to the manufacturer's instruction, 1000 ng extracted RNA was used to synthesize 20 μ l first strand cDNA (Revert aid™ first strand cDNA synthesis, Fermentas) of cDNA (500 ng) was used for PCR (Master Mix, 2 \times , Fermentas) using a thermo cycler (Bio RAD) for 35 cycles. As a negative control, cDNA was omitted from the reaction. The product size of PCR was analyzed by 2% agarose gel electrophoresis.

Real-time PCR. Real-time PCR was carried out with RNA from untreated and 400 mg/kg VPA-treated SCI groups. In both groups, 1,000 ng purified RNA (DNA free) from spinal cord and medulla oblongata was used to synthesize 20 μ l cDNA, using Revert aid™ first strand cDNA synthesis kit (Fermentas, Germany) as described above.

Table 1. Primer sequences and PCR parameters. Primers for amplification of target sequences, their Gen Bank accession number and size of the fragment amplified are presented.

Gene	Accession no.	Sense 5 → 3	Anti-sense 5 → 3	Size (bp)
BDNF	NM_012513	TTACACGAAGGAAGGCTGCAGG	ATGAACCGCCAGCCAATTCTC	122
GDNF	NM_019139	TATGGGATGTCGTGGCTGTCTG	TCGGGCATATTGGAGTCACTGG	157
B2M	NM_012512	CCCAACTTCTCAACTGCTACG	TTACATGTCTCGGTCCAGGTG	243
GAPDH	NM_008084	CAAGTCATCCATGACAACCTTG	GTCCACCACCCTGTTGCTGTAG	496

Primers were designed by Gene Runner 3.05 software (Product by: info@genfanavaran.com). BDNF, brain-derived neurotrophic factor; GDNF, glial cell-derived neurotrophic factor; B2M, beta-2-microglobulin; GAPDH, glyceraldehyde-3-phosphate dehydrogenase.

cDNA (500 ng) was used to quantify BDNF and GDNF mRNA levels. As an internal control, primers for beta-2-microglobulin (B2M) were used. All primers have been listed in Table 1. The PCR reaction was synthesized in a 25 μ l volume (sense and anti-sense primers, cDNA, Sybr green,) and carried out for 40 cycles (Applied Biosystems cycler). For analyzing relative changes in mRNA levels, we used the Pfaffl method (equation 1) [17]. GDNF and BDNF mRNA were normalized for B2M mRNA.

$$\text{Equation 1: } \Delta C_{t\text{target}} = C_{t\text{control}} - C_{t\text{treatment}} \text{ and } \Delta C_{t\text{reference}} = C_{t\text{control}} - C_{t\text{treatment}}$$

Histological quantitative analysis. Twenty eight days post injury, rats were killed and transcidentally perfused with 4% paraformaldehyde in PBS for five minutes. The lesion area was removed and post-fixed in 4% paraformaldehyde for another 12 h. Tissues were processed by an automatic processor (Leica TP1020) and embedded in paraffin. Serial section thickness (5 μ m) were prepared, dewaxed with chloroform and stained by hematoxylin/eosin [18]. Cell density per area, percentage of neural and glial cells, cavity and remaining tissue percentage were quantified by using ImageJ 1-44 software.

The total tissue and cavity volume (mm^3) in 3000 μ m length of the spinal cord (including rostral and caudal regions from the injury epicenter) were assessed for each sample. At first, serial section thickness (5 μ m) of spinal cord and cavity percentage, cell density and cell percentage were assessed in every twentieth section (totally 30 sections). The percentage of cavity and remaining tissue was calculated in 30 section using the Cavalieri method (equation 2, a, the measured area and d, the intersection distance) [19]. Serial summation of spared tissue and cavity volumes yielded the total volume of spared tissue. Any necrotic tissue within the cavities was counted as a part of the lesion and also any small cavity was calculated.

$$\text{Equation 2: } V_{sp} = a \times d$$

Neuroglial soma size was used for evaluation of cell percentage per area as follows: glial cells < 10 μ m; interneurons, γ -MN and sensory neurons > 10 μ m; α -MN > 25 μ m [20-23]. The numerical density per area and volume was used to evaluate the concentration of remaining cells (all cells including neuron and glial cells). For determination of cell density, equation 3 was used (N, the number of objects counted; A, the area and δ , the effective depth of field) [24].

$$\text{Equation 3: } D = \frac{N}{A\delta}$$

Immunohistochemistry. For immunostaining, sections were dewaxed by chloroform and hydrated with 100%, 96%, 70% ethanol and distilled water. Then, for inactivation endogenous peroxidase, sections were treated with 0.3% hydrogen peroxide in methanol for 15 min. The sections were preincubated in blocking solution (10% swine serum in TBS/BSA) at room temperature for 15 min and then incubated in primary antibodies at 4°C overnight (1:300 anti-MAP2 [microtubule-associated protein, Sigma], 1:100 anti-acetylated histone [H3, Serotec, USA] and 1:100 anti-ED1 [Serotec] monoclonal mouse IgG). Afterward, the sections were processed with avidin-biotin-HRP (ABC kit). Primary antibodies were visualized using the diaminobenzidine method. For counterstaining, the sections were stained by hematoxylin. Immunostainings were evaluated on three samples of each group. In each sample, three regions were considered for evaluation (rostral, center and caudal of lesion area). From each region, 5- μ m sections were prepared and five areas under 20 \times magnification were assessed (both ventral horn, both dorsal horn and central canal region). For evaluation, percentage of positive pixels per area in ED1 and MAP2 was quantified by Image J software.

Statistics. Statistical analysis was performed using SPSS15 software. All data are presented as means \pm SEM. To compare multiple means in groups, one-way ANOVA followed by Tukey's post hoc comparison was used. Values of $P < 0.05$ were considered statistically significant.

RESULTS

Behavioral assessment. The means of BBB scores of all groups have been compared in Figure 1. Rats were individually videotaped for four minutes at 3, 7, 14, 21 and 28 days post SCI. The means of BBB scores gradually increased at 7 days post injury. No significant difference was seen among the untreated-SCI group and VPA-treated groups on the 3 and 7 days post injury. At the other days, there was a significant difference among 200 and 400 mg/kg VPA-treated groups and other groups. Also, the means of BBB scores at 28 days post injury were significantly different between 400 and 200 mg/kg VPA-treated groups. The numerical difference (delta number) between day 3 and day 28 post injury was significantly different among 200 and 400 mg/kg VPA-treated groups and the other groups (Fig. 1B). In all groups, treatment by 400 mg/kg VPA until 28 days post injury was most efficient, with a delta number of 11.33 \pm 0.62.

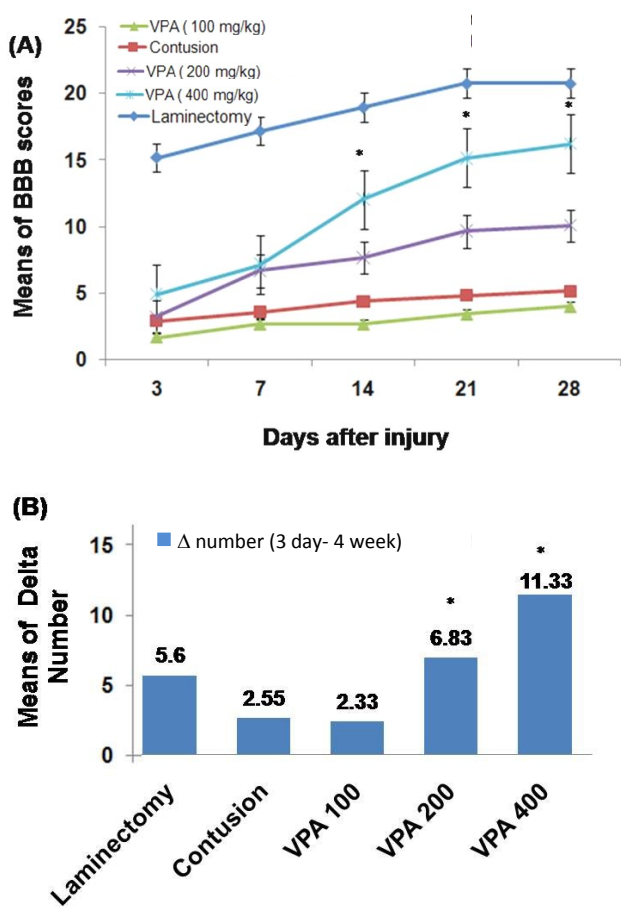


Fig. 1. Time course of open field Basso-Beattie Bresnahan (BBB) locomotor scores. The BBB scores were obtained starting from day 3 post injury until day 28 (5 time points). **(A)** Post hoc one-way ANOVA at 14, 21, 28 days post spinal cord injury revealed significant differences of 200 and 400 mg/kg VPA-treated groups as compared to 100 mg/kg VPA-treated and untreated-SCI groups. **(B)** Bar graph shows numerical difference (delta number) of BBB scores between day 3 and day 28 post injury. There are significant differences between groups treated with 200 and 400 mg/kg VPA as compared to the other groups. Bar graphs indicate the mean \pm SEM ($n = 6$) for each time point. * $P < 0.05$.

GDNF and BDNF genes expression. Increases of BDNF and GDNF Mrna levels in VPA-treated groups at day 28 post injury were confirmed by RT-PCR and quantitative real-time RT-PCR. The results of mRNA expression pattern have been shown in Figures 2 and 3. RT-PCR product electrophoresis showed 157 and 122 bp of GDNF and BDNF products, respectively. The brightness of product bands was measured using Image J software and results showed increasing thickness product band of both genes in the 400 mg/kg VPA-treated group as compared to the untreated-SCI group. In negative controls (without cDNA), no bands were detectable (Fig. 2). GDNF, BDNF mRNA real-time RT-PCR data showed that the expressions of BDNF and GDNF mRNA in 400 mg/kg VPA-treated group were significantly up-regulated in

comparison to the untreated-SCI group. The results demonstrate a significant increase of mRNA levels of both genes in the 400 mg/kg VPA group (4.76 ± 0.32 and 1.21 ± 0.6 fold change for BDNF and GDNF mRNA levels, respectively) (Figs. 3A, 3C and 3D).

Histological assessment and cavitation analysis. For evaluation of the therapeutic effects of VPA, histological assessments were performed at 28 days post injury. The percent of cavity in 3,000 μ m length of the injured spinal cord was evaluated using image J software. A significant difference between 400 mg/kg VPA-treated (0.61 ± 0.31) and -untreated (27.03 ± 5.23) groups (Fig. 4a) was observed. Most of the cavity is located at the epicenter of the lesion. The results demonstrate, from the center of the lesion rostrally and caudally, an increasing tissue density and a decreasing cavity percentage (Fig. 4C and 4D). The results demonstrate a significant decrease of numerical cells in gray and white matter of the rat spinal cord in untreated SCI group compared to the sham control and the 400 mg/kg VPA-treated groups, but there was no significant difference between the 400 mg/kg VPA-treated and the sham control groups (Fig. 4B). Results from neuronal and glial cell percentage in gray and white matter at 28 days post injury demonstrate a significant increase of glial cell and decreasing of neuronal cell percentage in untreated and VPA-treated groups compared to the sham control group (Fig. 5).

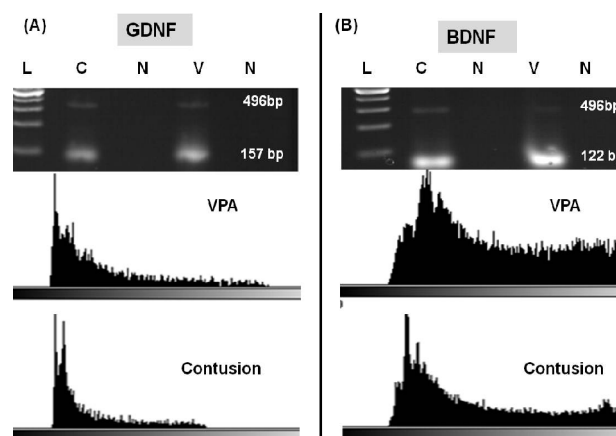


Fig. 2. Product analysis of RT-PCR for glial cell-derived neurotrophic factor (GDNF) and brain-derived neurotrophic factor (BDNF) and mRNA of 400 mg/kg Valproic acid (VPA)-treated (V) and -untreated groups (C) using RT-PCR and Image J software. **(A)** RT-PCR products of GDNF (122 bp). **(B)** RT-PCR products of BDNF (157 bp). Glyceraldehyde-3-phosphate dehydrogenase (496 bp) was used as a positive control of RNA integrity. The brightness of the product bands were measured using Image J software and results showed increasing thickness of product bands of both genes in 400 mg/kg VPA-treated group compared to the untreated spinal cord injury group. In negative controls (V) (without cDNA), no amplification products were seen. For sizing of fragments, a ladder of 200 bp and multiples was used.

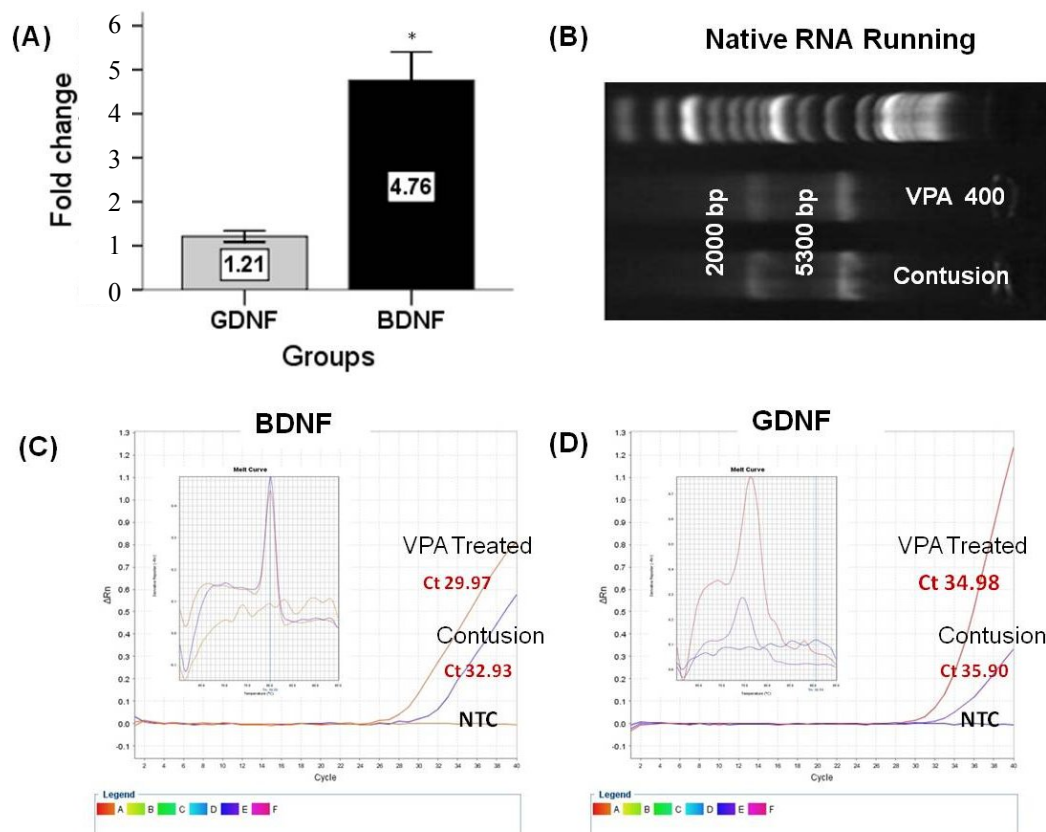


Fig. 3. Fold change ratio of glial cell-derived neurotrophic factor (GDNF) and brain-derived neurotrophic factor (BDNF) mRNA. Real-time PCR results are presented as relative expression normalized to B2M mRNA amplification. **(A)** Amplification of BDNF and GDNF mRNA derived from 400 mg/kg VPA-treated and -untreated groups 28 days post injury showing increased levels of both mRNA after 400 mg/kg VPA treatment. The results demonstrate significant differences between BDNF and GDNF mRNA levels. **(B)** Total RNA analyzed on a 1.5% denaturing agarose gel. The 18S and 28S ribosomal RNA bands were clearly visible in the intact RNA sample. **(C and D)** The amplification plot and melting curves for both amplification products. Bar graphs indicate the mean \pm SEM. * $P < 0.05$.

Results of quantification of glial and neuronal cells showed no significant difference between 400 mg/kg VPA-treated group and untreated-SCI group. We observed that the percentage of glial cells in 400 mg/kg VPA-treated group (67.89 ± 3.77) was decreased in comparison to the untreated-SCI group (77.13 ± 2.69), but the percentage of neuronal cells in 400 mg/kg VPA-treated group (32.10 ± 3.77) compared to untreated-SCI group (22.65 ± 2.69) was increased.

The effect of VPA on ED1 immunoreactivity. For evaluation of the effects of VPA on microglial and macrophage activation, ED1 (a lysosomal marker) immunostaining was used and analyzed with Image J by comparison of pixel density. A significant difference between immunopositive pixel (brown pixels) density between 400 mg/kg VPA-treated SCI (4.91 ± 1.12) and the untreated-SCI groups (19.94 ± 1.43) was observed. Also, the extension of the lesion area in the VPA-treated SCI group (0.06 mm^2) was significantly decreased as compared to the untreated-SCI group (0.58 mm^2) (Fig. 6).

The effect of VPA on neuronal dendrites growth.

For evaluating the effects of VPA on neuronal dendrite growth, MAP2 immunostaining and Image J software were used. In each group, three samples and in each sample three regions (rostral, center and caudal of lesion area) were analyzed. In each region, five areas (both ventral horns, both dorsal horns and central canal region) were assessed. The results demonstrated that administration of 400 mg/kg VPA significantly increased MAP2 positive immunoreactive pixels/area (43.02 ± 1.29 %) in comparison to the untreated-SCI group (24.26 ± 1.77 %). Also, there was significant difference between 400 mg/kg VPA-treated and sham control groups (75.08 ± 4.96 %) (Fig. 7).

The effect of VPA on H3 immunoreactivity.

For evaluation of the effects of VPA on global histone acetylation, H3 immunostaining (acetylated histone marker) and Image J software was used. The mean percentage of positive cells per area 28 days post SCI has been shown in Figure 8. Immunolabeled cells showed a brown staining of the nucleus (Fig. 8A and

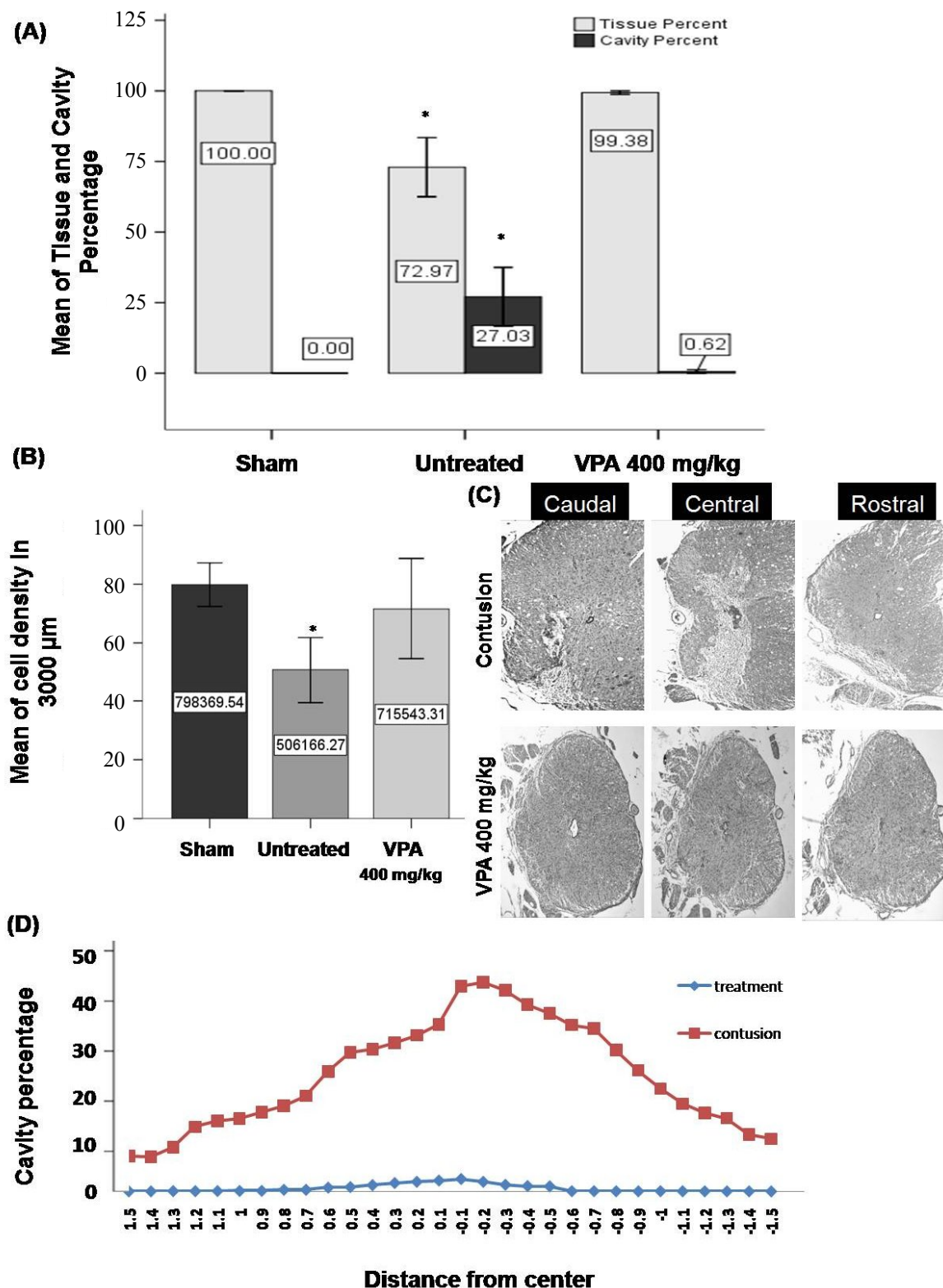


Fig. 4. Quantification of cell density and cavity percentage in gray and white matter 28 days post injury. (A and B) Means of cavity percentage (A) and cell density (B) in the 3000 μm length of injured spinal cord. Significant differences between 400 mg/kg VPA-treated and -untreated SCI groups, but not between the sham control and 400 mg/kg VPA-treated group. (C and D) Representative photomicrographs and line graphs showing the lesion extending from the epicenter rostrally end caudally. A massive destruction of gray matter and tissue loss at the epicenter in the untreated SCI group was seen in comparison to 400 mg/kg VPA-treated group. From epicenter to caudally and rostrally increase of tissue density and decrease of cavity percentage is seen. 4x magnification; Bar graphs indicate mean ± SEM; **P*<0.05 (untreated group compared to sham control and 400 mg/kg VPA groups).

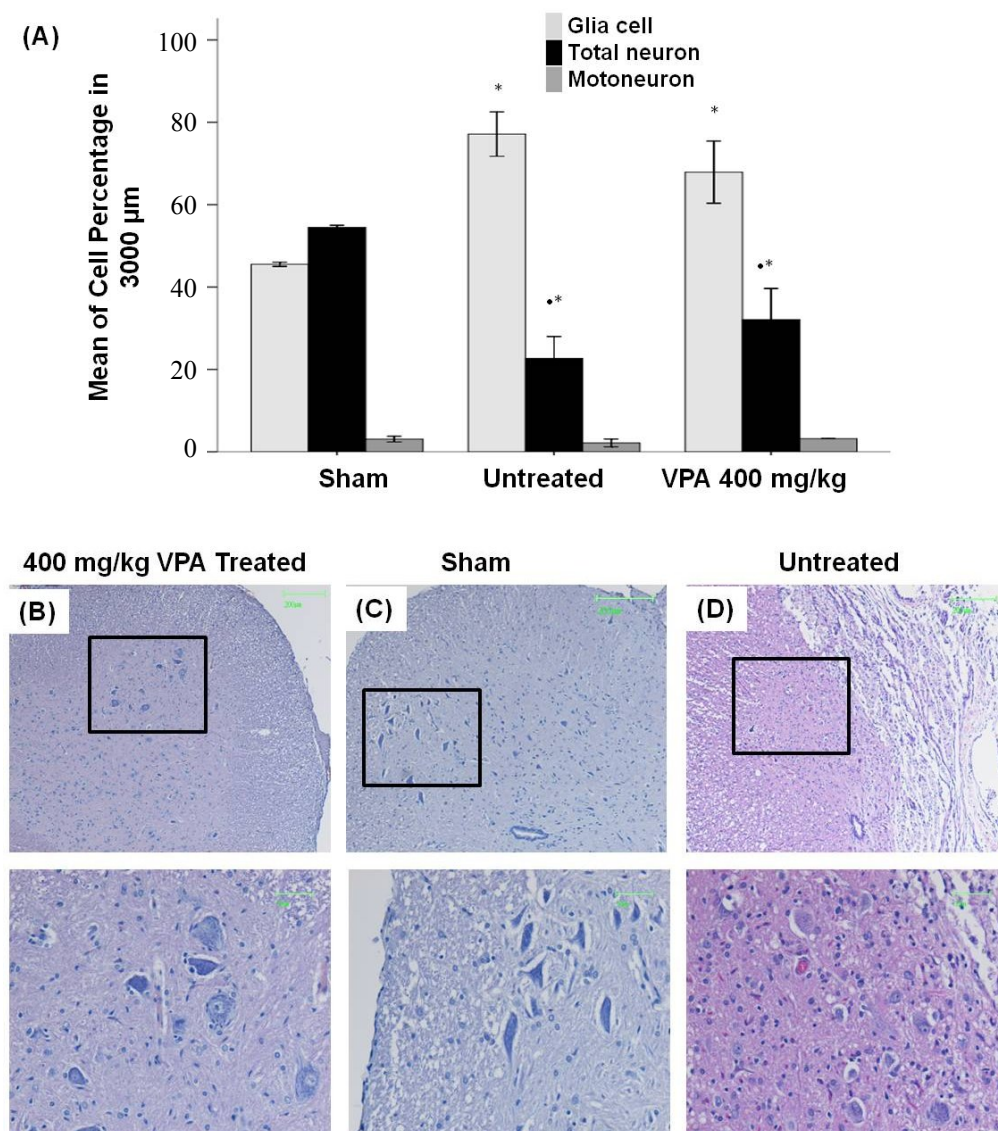


Fig. 5. Quantification of cell percentage in gray and white matter 28 days post injury. **(A)** Graph shows a significant increase of glial cells and decrease of neuronal cell percentages in untreated SCI and 400 mg/kg VPA-treated groups compared to the sham control group. **(B, C and D)** Representative hematoxylin/eosin stained photomicrographs showing the cell population in ventral horn of the spinal cord in VPA 400 mg/kg treated **(B)**, sham control **(C)** and untreated **(D)** groups. Scale bar 50 and 200 μ m; Bar graphs indicate the mean \pm SEM; * P <0.05 (compared to 400 mg/kg VPA groups); ** P <0.05 (compared to sham control group).

8C). There were no significant differences between 400 mg/kg VPA-treated ($71.61 \pm 3.15\%$) and the sham control group ($78.24 \pm 2.20\%$), but there were significant differences between the 400 mg/kg VPA-treated group compared to untreated-SCI group ($41.16 \pm 4.56\%$). Also, results demonstrated a significant difference between untreated groups compared to all other groups (Fig. 8D).

DISCUSSION

Secretions of proinflammatory cytokines from activated microglia and injured cells in earlier stage of

SCI exacerbate extend of lesion in chronic phase [25]. Loss of neurons, create cavity, disruption of axonal pathways and the formation of scar are the result of SCI in primary and secondary phases [26, 27].

In this study, therapeutic effects of different doses of VPA, a HDAC1 inhibitor, were studied in rat SCI. Histones acetylation is a key mechanism for modification of chromatin structure and gene expression [28]. Anti-inflammatory and neuroprotective effects of VPA in neurodegenerative condition were reported by many investigators [29-31]. In a model of ischemia, VPA treatment significantly decreased brain infarct volume, suppressed microglial activation, reduced the number of microglia, and

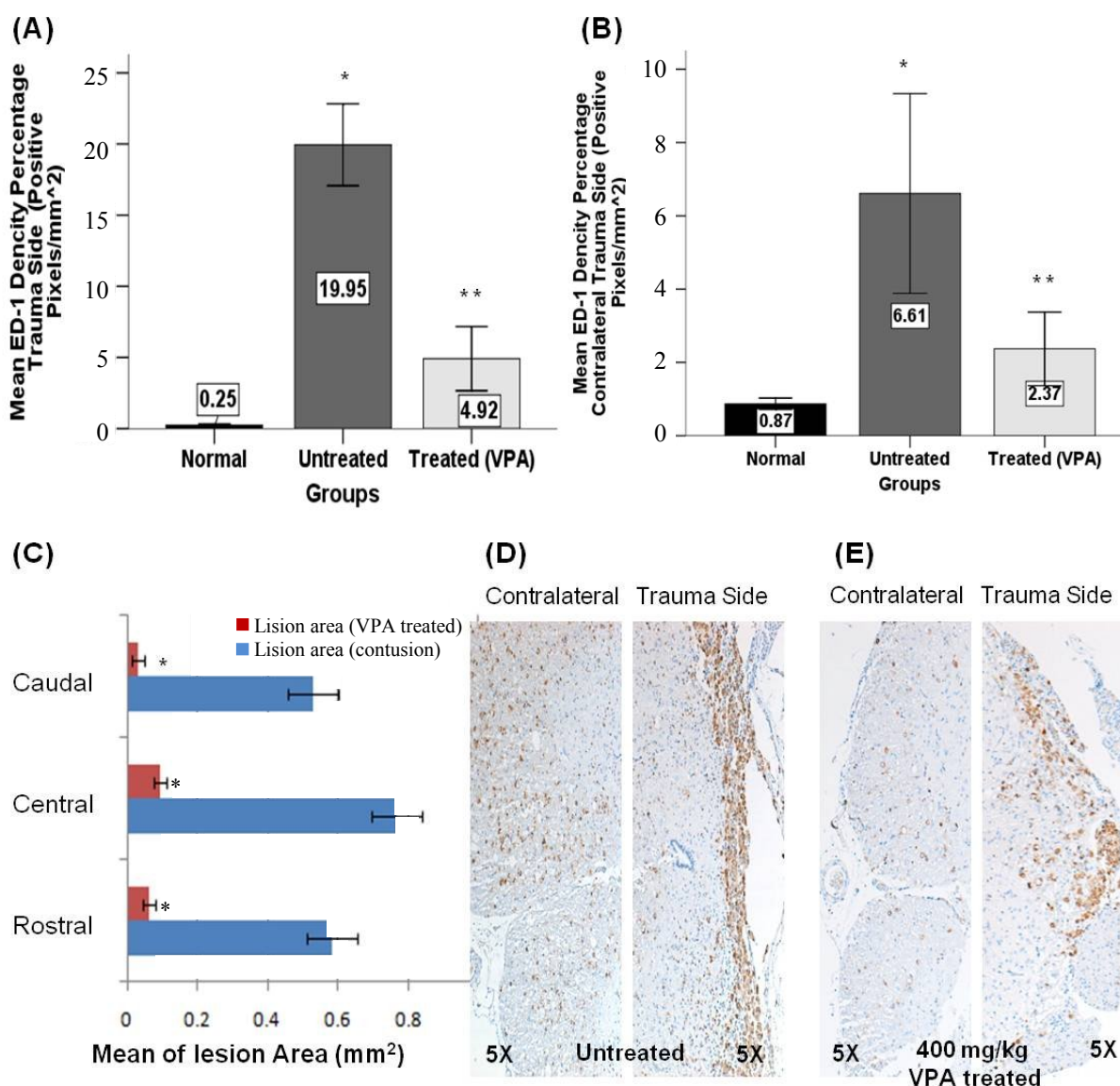


Fig. 6. Quantification of ED1 immunoreactivity 28 days post injury. (A and B) This graph shows the mean of positive pixel percentage at the lesion (above the central canal) (A) and in contralateral lesion side (below the central canal) (B). A significant difference between 400 mg/kg VPA-treated group compared to the untreated SCI and sham control groups was observed. (C) A significant difference between the mean sizes of the lesion area was seen for all groups and all regions. (D and E) Representative photomicrographs of ED1 immunoreactivity at the lesion side and contralateral of untreated SCI (D) and 400 mg/kg VPA-treated groups (E). Graphs indicate the mean \pm SEM; ** $P < 0.05$ (compared to the sham control and untreated SCI groups); * $P < 0.05$ (compared to the sham control and VPA 400 mg/kg groups).

inhibited other inflammatory markers in the ischemic brain [32]. VPA treatment suppressed mRNA expression of a variety of cytokines that are important in regulating inflammation. Our results show that the best dose of VPA treatment is 400 mg/kg and the percentage of ED1 positive cells, compared to the untreated group, was significantly decreased. This data is in accordance with that of Bhavsar *et al.* [33].

Neurotrophic factors are key nervous system regulatory proteins that modulate neuronal survival, axonal growth, synaptic plasticity and neurotransmission. A study showed that *in vitro*

condition treatment of neurons with valproic induces neurite outgrowth [34]. Administration of VPA in *in vivo* condition enhances hippocampal neurogenesis [35] and has protective effects on dopaminergic neurons in midbrain neuron [36]. For evaluation VPA effects on neuritis outgrowth, we checked MAP-2 and our results demonstrated that there is a significant difference between 400 mg/kg VPA group compared to untreated group.

We observed that VPA (400 mg/kg) greatly reduced the development of secondary damage in rat spinal cord trauma; resulting into better locomotor scores and

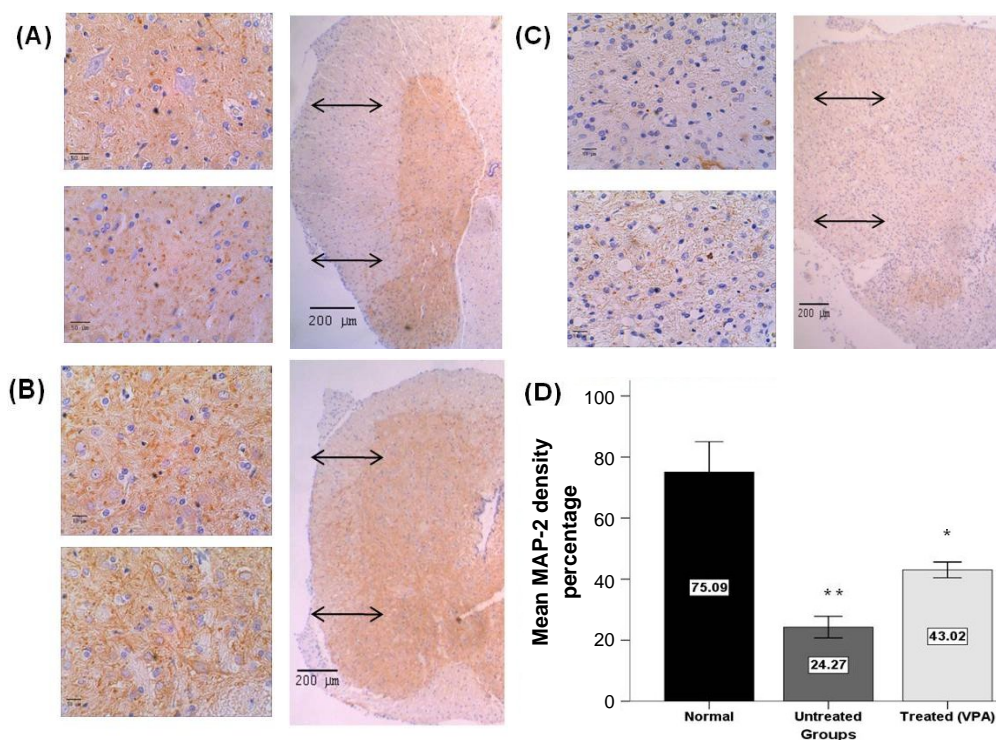


Fig. 7. Quantification of MAP2 immunoreactivity 28 days post injury. Representative photomicrographs showing MAP-2 immunoreactivity in ventral and dorsal horns of the spinal cord of sham control (A), VPA 400 mg/kg treated (B) and untreated SCI (C) groups. The brown pixels are immunopositive and the blue pixels are hematoxylin staining. (D) Percentage of MAP2 positive pixels. A significant difference between 400 mg/kg VPA treated, untreated SCI and sham control groups were observed. Scale bar 50 and 200 μm ; Graphs indicate the mean \pm SEM; ** $P < 0.05$ (compared to the sham control and 400 mg/kg VPA groups); * $P < 0.05$ (compared to sham control and untreated SCI groups).

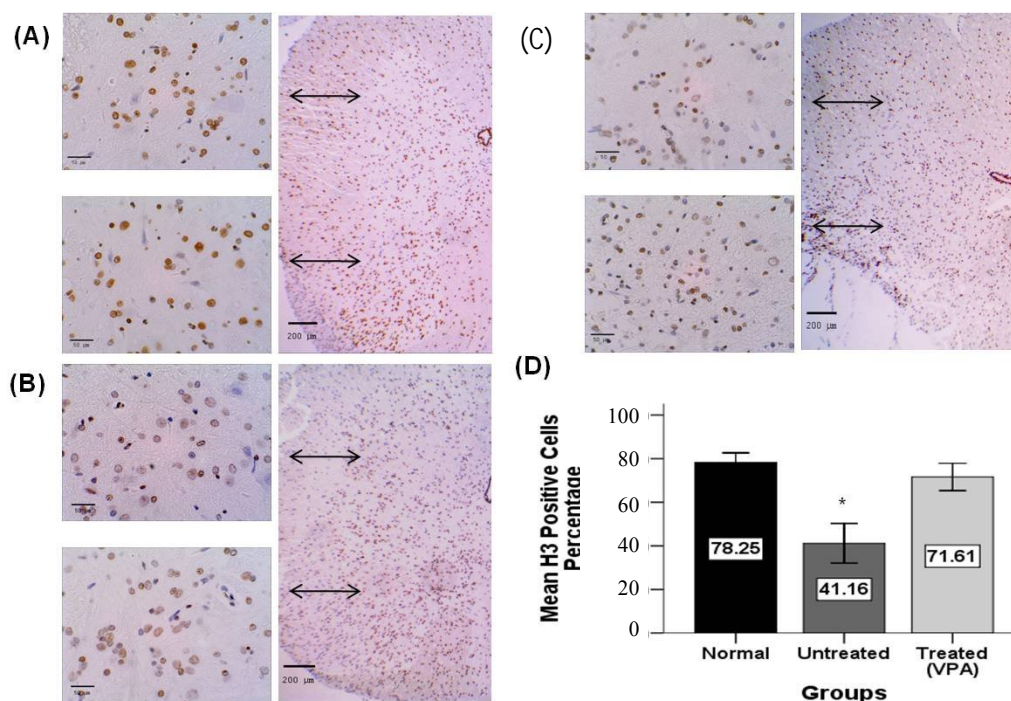


Fig. 8. Quantification of acetylated histone (H3) immunoreactivity 28 days post injury. Representative photomicrographs showing H3 immunoreactivity in ventral and dorsal horn spinal cord areas of sham control (A), VPA 400 mg/kg treated (B) and untreated SCI groups (C). The brown nuclei are immunopositive and are counterstained by hematoxylin (blue). (D) Graph showing the percentage of H3 positive cells. There is no significant difference between VPA treated and sham control groups, but there is significant difference between the 400 mg/kg VPA treated and the untreated SCI group. Scale bar 50 and 200 μm ; Graphs show mean \pm SEM; * $P < 0.05$ (compared to the sham control and 400 mg/kg VPA treatment groups).

more rapid recovery. Also, VPA administration increased regional BDNF and GDNF mRNA levels. Local inflammation and the expression of the lysosomal marker ED1 by activated macrophages/microglial cells were reduced by VPA and immunoreactivity of H3 and MAP2 increased.

VPA is a promising drug candidate in the treatment of SCI and most probably other traumatic injuries to the central nervous system. It is a cheap drug, clinically used in the treatment of various neurologic diseases, such as epilepsy, migraine or mood disorders. VPA is an HDAC1 inhibitor that could be used for treatment of many diseases; however, VPA has a few other targets in the organs of body, which might contribute to its effects in SCI.

ACKNOWLEDGMENTS

We are grateful to Mr. Ali Norizadeh, Mehri Fayazi, Zhiyuan Zhang and Caroline Zug for their excellent technical assistance and advice. This work was supported, in part, by a research grant from the Shafa Neuroscience Center, Khatam Al-Anbia hospital, Tehran, Iran.

REFERENCES

- Donnelly DJ, Popovich PG. Inflammation and its role in neuroprotection, axonal regeneration and functional recovery after spinal cord injury. *Exp Neurol*.2008 Feb;209(2):378-88.
- Chen PS, Peng GS, Li G, Yang S, Wu X, Wang CC et al. Valproate protects dopaminergic neurons in midbrain neuron/glia cultures by stimulating the release of neurotrophic factors from astrocytes. *Mol Psychiatry*.2006 Dec;11(12):1116-25.
- Castro LM, Gallant M, Niles LP. Novel targets for valproic acid: up-regulation of melatonin receptors and neurotrophic factors in C6 glioma cells. *J Neurochem*.2005 Dec; 95(5):1227-36.
- Glauben R, Batra A, Fedke I, Zeitz M, Lehr HA, Leoni F et al. Histone hyperacetylation is associated with amelioration of experimental colitis in mice. *J Immunol*.2006 Apr; 176(8):5015-22.
- Balbi A, Sottofattori E, Mazzei M, Sannita WG. Study of bioequivalence of magnesium and sodium valproates. *J Pharm Biomed Anal*.1991;9(4):317-21.
- Brandt C, Gastens AM, Sun M, Hausknecht M, Löscher W. Treatment with valproate after status epilepticus: effect on neuronal damage, epileptogenesis, and behavioral alterations in rats. *Neuropharmacology*.2006 Sep;51(4):789-804.
- Zhang Z, Zhang ZY, Fauser U, Schluesener HJ. Valproic acid attenuates inflammation in experimental autoimmune neuritis. *Cell Mol Life Sci*.2008 Dec;65(24):4055-65.
- Yuan PX, Huang LD, Jiang YM, Gutkind JS, Manji HK, Chen G. The mood stabilizer valproic acid activates mitogen-activated protein kinases and promotes neurite growth. *J Biol Chem*.2001 Aug;276(34):31674-83.
- Gurvich N, Klein PS. Lithium and valproic acid: parallels and contrasts in diverse signaling contexts. *Pharmacol Ther*.2002 Oct;96(1):45-66.
- Hao Y, Creson T, Zhang L, Li P, Du F, Yuan P et al. Mood stabilizer valproate promotes ERK pathway-dependent cortical neuronal growth and neurogenesis. *J Neurosci*. 2004 Jul;24(29):6590-9.
- Bose P, Parmer R, Thompson FJ. Velocity-dependent ankle torque in rats after contusion injury of the midthoracic spinal cord: time course. *J Neurotrauma*.2002 Oct; 19(10): 1231-49.
- Ohta M, Suzuki Y, Noda T, Ejiri Y, Dezawa M, Kataoka K et al. Bone marrow stromal cells infused into the cerebrospinal fluid promotes functional recovery of the injured rat spinal cord with reduced cavity formation. *Exp Neurol*.2004 Jun;187(2):266-78.
- Khalatbary AR, Tiraihi T. Localization of bone marrow stromal cells in injured spinal cord treated by intravenous route depends on the hemorrhagic lesions in traumatized spinal tissues. *Neurol Res*.2007 Jan;29(1):21-6.
- Dash PK, Orsi SA, Zhang M, Grill RJ, Pati S, Zhao J et al. Valproate administered after traumatic brain injury provides neuroprotection and improves cognitive function in rats. *PLoS One*.2010 Jun; 5(6):e11383.
- Basso DM, Beattie MS, Bresnahan JC. Graded histological and locomotor outcomes after spinal cord contusion using the NYU weight-drop device versus transection. *Exp Neurol*.1996 Jun;139(2):244-56.
- Zhang Y, Wang J, Chen G, Fan D, Deng M. Inhibition of Sirt1 promotes neural progenitors toward motoneuron differentiation from human embryonic stem cells. *Biochem Biophys Res Commun*.2011 Jan;404(2):610-4.
- Yuan JS, Reed A, Chen F, Stewart CN Jr. Statistical analysis of real-time PCR data. *BMC Bioinformatics*.2006 Feb;7:85.
- Llewellyn BD. Nuclear staining with alum hematoxylin. *Biotech Histochem*.2009; 84(4):159-77.
- Parr AM, Kulbatski I, Zahir T, Wang X, Yue C, Keating A et al. Transplanted adult spinal cord-derived neural stem/progenitor cells promote early functional recovery after rat spinal cord injury. *Neuroscience*.2008 Aug;155(3): 760-70. Epub 2008 Jun 5.
- Zhou W, Ge WP, Zeng S, Duan S, Luo Q. Identification and two-photon imaging of oligodendrocyte in CA1 region of hippocampal slices. *Biochem Biophys Res Commun*. 2007 Jan;352(3):598-602.
- Sasaki T, Kuga N, Namiki S, Matsuki N, Ikegaya Y. Locally synchronized astrocytes. *Cereb Cortex*.2011 Aug; 21(8):1889-900.
- Sergeeva OA, Fleischer W, Chepkova AN, Warskulat U, Häussinger D, Siebler M et al. GABAA-receptor modification in taurine transporter knockout mice causes striatal disinhibition. *J Physiol*.2007 Dec; 585(Pt 2):539-48.
- Wei IH, Tu HC, Huang CC, Tsai MH, Tseng CY, Shieh JY. (-)-Epigallocatechin gallate attenuates NADPH-d/nNOS expression in motor neurons of rats following peripheral nerve injury. *BMC Neurosci*.2011 Jun; 1:12:52.
- McLaren JW, Bourne WM, Patel SV. Automated assessment of keratocyte density in stromal images from the ConfoScan 4 confocal microscope. *Invest Ophthalmol Vis Sci*.2010 Apr;51(4):1918-26.
- Fleming JC, Norenberg MD, Ramsay DA, Dekaban GA, Marcillo AE, Saenz AD et al. The cellular inflammatory response in human spinal cords after injury. *Brain*.2006

- Dec;129(Pt 12):3249-69.*
26. Beattie MS, Li Q, Bresnahan JC. Cell death and plasticity after experimental spinal cord injury. *Prog Brain Res.*2000;128:9-21
 27. Fehlings MG, Nguyen DH. Immunoglobulin G: a potential treatment to attenuate neuroinflammation following spinal cord injury. *J Clin Immunol.*2010 May;30 Suppl1:S109-12.
 28. Bhavsar P, Ahmad T, Adcock IM. The role of histone deacetylases in asthma and allergic diseases. *J Allergy Clin Immunol.*2008 Mar;121(3):580-4.
 29. Kim HJ, Rowe M, Ren M, Hong JS, Chen PS, Chuang DM. Histone deacetylase inhibitors exhibit anti-inflammatory and neuroprotective effects in a rat permanent ischemic model of stroke: multiple mechanisms of action. *J Pharmacol. Exp Ther.*2007 Jun;321(3):892-901.
 30. Sinn DI, Kim SJ, Chu K, Jung KH, Lee ST, Song EC et al. Valproic acid-mediated neuroprotection in intracerebral hemorrhage via histone deacetylase inhibition and transcriptional activation. *Neurobiol Dis.*2007 May;26(2):464-72.
 31. Watterson JM, Watson DG, Meyer EM, Lenox RH. A role for protein kinase C and its substrates in the action of valproic acid in the brain: implications for neural plasticity. *Brain Res.*2002 Apr;934(1):69-80.
 32. Kim HJ, Rowe M, Ren M, Hong JS, Chen PS, Chuang DM. Histone deacetylase inhibitors exhibit anti-inflammatory and neuroprotective effects in a rat permanent ischemic model of stroke: Multiple mechanisms of action. *J. Pharmacol. Exp Ther.*2007;321(3):892-901.
 33. Bhavsar P, Ahmad T, Adcock IM. The role of histone deacetylases in asthma and allergic diseases. *J. Allergy Clin. Immunol.*2008;121:580-4.
 34. Yuan PX, Huang LD, Jiang YM, Gutkind JS, Manji HK. The mood stabilizer valproic acid activates mitogen-activated protein kinases and promotes neurite growth. *J Biol Chem.* 2001;276:31674-83.
 35. Hao Y, Creson T, Zhang L, Li P, Du F. Mood stabilizer valproate promotes ERK pathway-dependent cortical neuronal growth and neurogenesis. *J Neurosci.*2004;24:6590-9.
 36. Chen PS, Peng GS, Li G, Yang S, Wu X, Wang CC et al. Valproate protects dopaminergic neurons in midbrain neuron/glia cultures by stimulating the release of neurotrophic factors from astrocytes. *Mol Psychiatry.*2006; 11:1116-25.